Electronic structure and surface kinetics of palladium hydride studied with x-ray photoelectron spectroscopy and electron-energy-loss spectroscopy

P. A. Bennett* and J. C. Fuggle
Institut für Festkörperforschung, Kernforschungsanlage Jülich, West Germany
(Received 11 June 1982)

X-ray photoelectron spectra and electron-energy-loss spectra (EELS) are presented and interpreted for $PdH_{\sim 0.8}$ prepared by *in situ* loading and cleaning of a 10-μm foil cooled to 80 K. Hydrogenation induces new states with considerable *d* character 8 eV in the valence band, a slight narrowing of the valence-band spectrum, and a shift of the Fermi level out of the *d* manifold of states. In the core-line spectra a +0.17-eV binding-energy shift occurs, the asymmetry is reduced, and a shake-up satellite at 6 eV essentially disappears. In the EELS spectra a 7-eV plasmon loss is attenuated and shifted to 5 eV. During degassing experiments, no significant surface depletion is found, and two different rates occur: For concentrations $H_x \gtrsim 0.65$ atomic fraction hydrogen (β phase) an activation energy of 8.1-kcal/mole H_2 is found, while for $H_x \gtrsim 0.65$ (two-phase region) the rate is 10^5 slower, but has a similar activation energy of 9.0-kcal/mole H_2. During this time the surface contains both β and α phases.

I. INTRODUCTION

In this paper we present and interpret x-ray photoemission spectra (XPS) and electron-energy-loss spectra (EELS) for palladium hydride, and investigate the role of the surface in the kinetics of degassing. Photoemission and reflectivity experiments combined with band-structure calculations for several "high-temperature" materials such as ThH_2, Th_4H_{15}, ScH_2, and LaH_2 have demonstrated the inadequacy of the early "rigid-band" models for hydrides.[1-3] The use of ultrahigh vacuum (UHV) techniques to study palladium hydride, however, has been hindered by the relatively high equilibrium pressure of ~ 10 Torr at room temperature. In the present experiments we achieve a clean, well-characterized surface by *in situ* loading and cleaning and by cooling of the sample.

In early uv photoemission experiments on palladium hydride, hydrogen-induced states in the valence-band spectrum were reported at 5.4 eV, which agreed with band-structure calculations given in the same publication.[4] This was the first such comparison for any metal hydride and was important in signaling the inadequacy of the "rigid-band" models. However, more recent calculations place the hybridized bonding states near 8 eV,[5-7] and the early experimental results have been questioned.[8-10] The core-level spectra are of interest because one has information (at least indirectly) regarding charge transfer to or from the palladium site. Valence-band information can also be inferred from the core-level line shape since the incomplete occupation of the *d* bands give rise to a discrete shake-up satellite at 6 eV, analogous to the well-known case of nickel,[11-16] and a continuous tail of intensity at lower kinetic energy.[17,18] Core-level spectra for a series of electrolytically charged samples showed an apparently sudden broadening of the line for hydrogen concentrations below $H_x = 0.7$. This was interpreted to result from the Fermi level entering the *d* bands at this concentration.[19] There are reflectivity and energy-loss data as well as calculated dielectric functions for palladium, but not for the hydride.[20-22]

The kinetics of hydrogen uptake and release are a major factor in the utilization of hydrides as storage materials, and this is known to vary greatly with surface conditions.[23] Palladium is unique in that its surface remains relatively clean and permeable to hydrogen. Indeed, it is sometimes used as a permeation coating for other materials which otherwise form a "sealing oxide surface layer."[24] It also does not decrepitate upon loading, as the commercially important $LaNi_5$ or FeTi alloys do.[25] For these reasons it is an ideal system in which to study the intrinsic kinetic behavior. Several experiments have reported that the reaction $2H \leftrightarrow H_2$ taking place at

or near the surface with an activation energy of $\sim$7-kcal/mole H_2 is the rate-limiting step both for the uptake and release of hydrogen, at least under certain "typical" conditions.[26,27] These experiments were only for dilute concentrations. In the present experiments, we can monitor the hydrogen concentration near the surface and the rate of degassing as the fully loaded sample is warmed. This technique has the important advantages that it is steady state, requiring no input regarding surface-site occupation or its time variation, and it allows measurements with concentrated samples.

II. EXPERIMENTAL APPARATUS AND TECHNIQUE

The XPS machine was a custom-built Kratos instrument modified by the addition of a large solid-angle monochromator. For these experiments the energy resolution was 0.6 eV full width at half maximum (FWHM). A special feature of the vacuum apparatus was a Leybolt-Hereaus preparation chamber which allowed exposure of the sample to pressures up to 10 atm, control of temperatures from 80 to 850 K, and transfer of the sample under vacuum into the measuring chamber.

The sample was a (1×1 cm$^2\times10$ μm)-thick palladium foil of 99.99% purity from W. Hereaus. After a washing in methanol and acetone, it was mounted alongside a reference gold foil by screwing its corners to the support stage. Surface contamination was monitored using XPS core-level intensities and was removed by ion bombardment. This resulted in a valence-band spectrum characteristic of clean palladium.[28] After the initial surface cleaning, the sample was loaded under 2000-Torr pressure for 20 min at 400 K, and then cooled under pressure at $\sim$10 °C/min to 80 K. The resulting concentration can be estimated from the palladium-hydrogen phase diagram which is shown in Fig. 1.[29] For temperatures above the "50-K anomaly" there are only two phases, α and β, with a cosolute temperature of 570 K corresponding to 20 atm pressure and $H_x=0.25$.[30] The initial 20 min of our loading allows for the slow transformation through the two-phase region to a concentration of $H_x\sim0.64$. (Subsequent volumetric calibration showed that 20 min was certainly enough to allow β-phase formation since the same total hydrogen uptake resulted with only 10 min waiting.) As the sample cools under pressure, the hydrogen concentration increases, following the 2000-Torr isobar until the slowing kinetics prevent further uptake. Using our data on the kinetics for this sample, we estimate the resulting concentration to be $H_x=0.80\pm0.10$. We mention here in anticipation of later discussion that during degassing one may expect to find a changing behavior as H_x first decreases to the boundary of the two-phase region, whose limits at 200 K are $H_x^{\beta}=0.64$ and $H_x^{\alpha}\approx0$, and subsequently crosses through the two-phase region, where particles of β-phase material convert to the α phase.

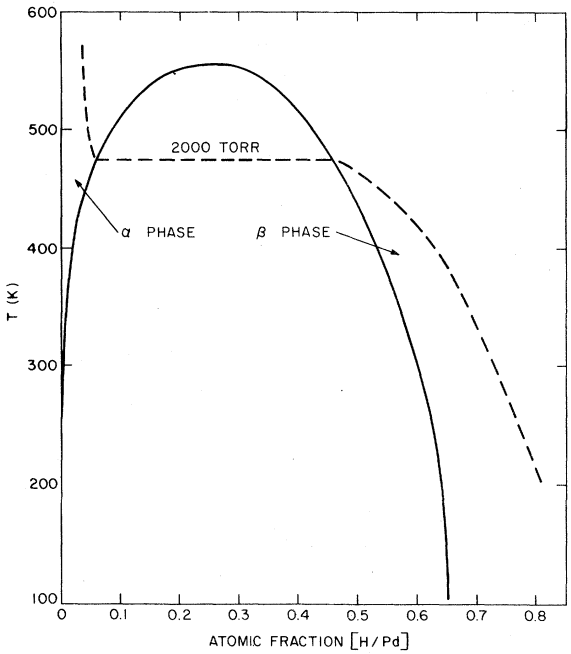

FIG. 1. Phase diagram of the palladium-hydrogen system. The 2000-Torr isobar is shown as a dotted line and indicates that a concentration of $H_x\sim0.80$ is achieved.

The fully loaded sample was then introduced into the measuring chamber where a background pressure of $\sim2\times10^{-10}$ Torr (principally atmospheric gases leaking past the sliding seals) was obtained. The XPS spectra of the loaded, cold sample showed emission from oxygen and carbon core levels corresponding to O=0.16 and C=0.14 atomic fractions relative to palladium. This was calculated using atomic photoionization cross sections for the O 2*s*, C 1*s*, and Pd 3*d* levels.[31] Attempts to remove these contaminants by ion sputtering or scraping gave levels of O=0.13 and C=0.20, or 0.20 and 0.10, respectively. It was found, however, that briefly warming the sample to 100 K reduced these to $O\leq0.03$ and C=0.14, which were the same as obtained for the ion-sputtered pure palladium sample.

The preferred treatment was therefore no cleaning except for a series of "flashings" to remove weakly adsorbed contaminants. Removal of these contaminants produced no noticeable change in the valence-band, core-level, or EELS spectra. We also measured these spectra after exposing the cleaned, cold (120 K) sample to ~ 1000 L of H_2 or 1000 L (1 L = 1 langmuir = 10^{-6} Torr sec) of atmospheric gases and again found no noticeable change. We conclude that the presence of surface-adsorbed oxygen or carbon (approximately less than one monolayer) had no significant effect on the spectra, and presume this is due to the relatively long mean free path for escaping electrons, which have therefore little surface sensitivity. XPS investigations have previously shown that a monolayer of chemisorbed gas has little effect on the core-level and valence-band spectra from metal substrates and that such effects are only observed at grazing angles. Much larger effects occur, however, if the contaminant forms a true compound at the surface.[32–34] The spectra shown for the dehydrided sample were measured at 220 K, a temperature just sufficient to desorb hydrogen from the bulk after several hours waiting.

The Fermi level was located by positioning the sample such that signals from palladium and gold could both be recorded without moving the sample. The measurements were then repeated after degassing. This procedure for locating the Fermi level was necessary to accommodate variations of the analyzer work function found to occur with higher hydrogen pressures in the measuring chamber.

After measuring spectra for the fully hydrided and degassed samples, a series of loading and degassing runs were made in order to characterize the kinetics and to determine the concentration of hydrogen in the surface region. "Surface region" in this case means the escape depth for electrons of ~ 1500-eV energy, which is ~ 20 Å. The hydrogen concentration averaged over the bulk H_x^{bulk} is monitored by the time-integrated pressure of hydrogen escaping into the pumped chamber, while the surface concentration H_x^{surf} is monitored by the behavior of the XPS and EELS spectra. Later we will interpret the pressure P to be proportional to the rate of release of H_2 molecules from the sample, and interpret its normalized time integral,

$$n(t)=\frac{\int_0^t P(t',T)\,dt'}{\int_0^\infty P(t',T)\,dt'},$$

to be the fraction of gas that has been desorbed from the sample. Two observations substantiate this procedure: The total gas pumped is independent of the temperature (thus rate) of the degassing, and the computed pumping speed assuming an initial bulk concentration of $H_x=0.80$ agrees within our uncertainty (a factor $2\times$) with the manufacturer's value. At the end of degassing runs, a residual pressure of $\sim 3\times 10^{-10}$ Torr remained for long periods of time. This was presumably due to wall-released gases or saturation of the pumps and was subtracted out for the Arrhenius plots shown later.

III. RESULTS AND INTERPRETATION

A. Electronic structure

The valence-band spectra are shown in Fig. 2 for the fully hydrided and degassed samples. The intensity scale is arbitrary, while the energy scale is determined using the gold reference. As discussed later, we find that the hydrogen concentration in the surface region is approximately equal to that in the bulk, which is $H_x=0.80$. The following changes are observed upon hydrogenation: New states appear around 8-eV binding energy (BE), the Fermi level moves such that the half maximum near the top of the valence band is at 0.16 ± 0.05 eV lower kinetic energy (KE), the total width of the d bands is decreased $\sim 10\%$, and a small peak appears near the top of the band.

The spectra of the palladium $3d$ core levels are shown in Fig. 3 again, for the fully hydrided and dehydrided samples. The main peak heights have

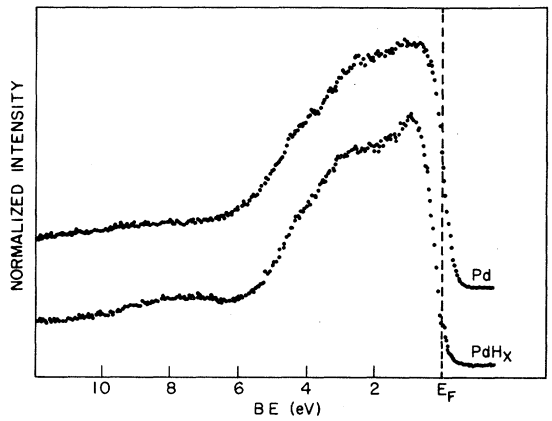

FIG. 2. XPS valence-band spectra for the fully hydrided and subsequently degassed samples. The Fermi level is calibrated with a gold reference.

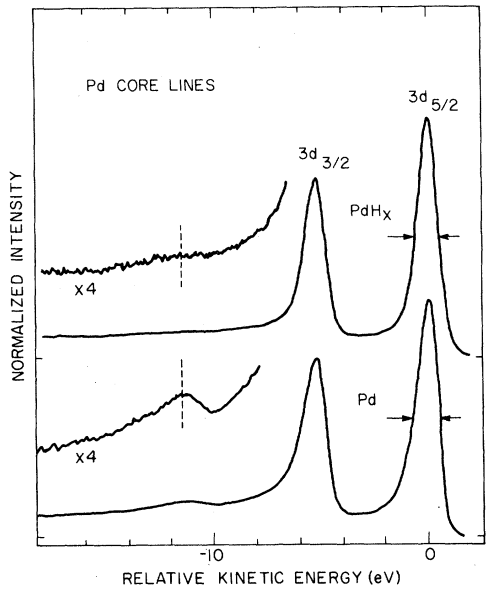

FIG. 3. Core-level spectra of the $3d_{5/2}$ and $3d_{3/2}$ lines for the fully hydrided and degassed samples. The main peaks have been aligned, so the $+0.17$-eV chemical shift for the hydride is not shown. Arrows mark the FWHM which decreases from 1.45 to 1.20 eV (instrumental solution ~ 0.6 eV). A dotted line marks a satellite of the $3d_{3/2}$ line which disappears in the hydride.

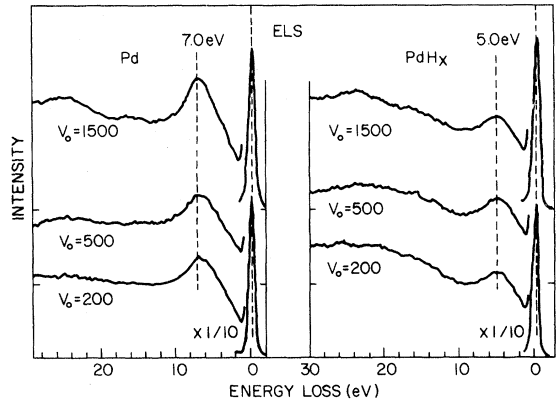

FIG. 4. EELS spectra of nearly fully hydrided (the surface cleaning reduced the hydrogen concentration to $H_x \sim 0.7$ for these spectra) and depleted samples for several different primary beam energies. The intensity scale is normalized to the elastic peak in all cases. The plasmon-loss feature, marked with a dotted line, is seen to shift from 7.0 to 5.0 eV in the hydride.

been drawn equal and the energy scale has been adjusted to align the peaks. Upon hydrogenation, the satellite feature present at 6 eV below each of the spin-orbit-split lines is seen to essentially disappear, and the lines become less asymmetric, which reduces their measured FWHM from 1.45 to 1.20 eV. Not shown on the drawing is a 16% decrease of the peak maximum corresponding to a 20% reduction in integrated intensity. Also, the energy of the half maximum on the high-KE side of the line decreases $0.17 \pm .05$ eV with respect to the gold reference lines.

The EELS data are shown in Fig. 4 for several different primary beam energies. The vertical scale has been normalized to the elastic peak intensity for all traces. In pure palladium, a prominent peak is present at 7-eV energy loss, followed by a weaker and much broader peak around 25 eV. This structure does not change much at lower primary energies, except that a shoulder appears on the smaller loss side of the 7-eV peak. In the hydride spectra the 7-eV peak is shifted to ~ 5.0 eV and reduced in intensity by $\frac{1}{2}$, and the broad structure near 25 eV appears somewhat larger. Again, little variation is seen with decreasing primary energy. The lack of sensitivity to primary beam energy indicates that surface states or possible surface contamination contribute little to the spectra. Not shown in the drawing is a 40% decrease of the elastic peak intensity at 1500 eV for the hydrided sample. This may result from a reduction in the mean free path of the electrons. The same mechanism would also cause the observed reduction of the photoemisson peaks, but by only $\sim \frac{1}{2}$ of the 40%, since in the latter case the distribution of "primary" electrons is uniform over the range of the escape depth.

Our measured valence-band spectrum is in good qualitative agreement with several recent bulk band-structure calculations for the palladium-hydrogen system.[5–7] The new states at 8 eV are strongly hybridized bonding orbitals between the palladium and hydrogen atoms. The fact that they are visible with x-ray excitation demonstrates that considerable d character remains in these states, since the photoemission cross section for the H $1s$ atomic orbital is 10^{-5} that of the palladium $4d$ orbitals.[25] The narrowing of total bandwidth may result from the 3% increase of the lattice parameter upon hydrogenation, or from a reduction of lifetime broadening due to filling of the d bands. The reduced density of states at the Fermi energy is consistent with the changes in electronic specific heat and magnetic susceptibility,[29] as well as band-structure calculations for nonstoichiometric concentrations.[7] The increased intensity found near the top of the bands is not present in the calculations, but is presumed to result from an instrumental broadening which obscures the peak in pure palladi-

um and enhances the peak in the hydride, where it is further below the Fermi cutoff. Our spectrum appears different from early ultraviolet photoemission spectroscopy (UPS) spectra,[4] which reported new states at 5.4-eV BE. The discrepancy may result from surface contamination, an enhanced sensitivity to true surface states,[35,36] structure in the final density of states (DOS), or matrix-element variations across the band. Presumably none of these affect our XPS spectra appreciably.

We interpret the change in the core-level line shape to result from a filling of the valence-band d orbitals upon hydrogenation and the subsequent decrease to nearly zero of the DOS at E_F. This follows since the satellite and shake-up tail are understood to result from empty d states just above the Fermi level, analogous to the case of nickel and its alloys.[14–16] [There is a possibility in the case of pure palladium that some intensity in the region of the satellite arises through inelastic scattering (see next paragraph).] The disappearance of the satellite, however, does not necessarily indicate a charge transfer to palladium sites as implied by the old "protonic" model or the description of "band filling." Similarly, the chemical shift of $+0.17\pm0.05$ eV (increased BE) observed in the hydride suggests that the hydrogen proton is "overscreened" in the solid. However, in view of the difficulty of relating BE shifts to ground-state properties, we caution against a simplistic picture of charge transfer to the proton, particularly for such a small shift.

Our interpretation of the energy-loss spectra is guided by similarity of the pure metal spectra to the reported energy-loss function for bulk palladium.[20–22] Thus we assign the 7-eV feature to a plasmon loss ($\epsilon_1=0, \epsilon_2\sim 2$) and the 25-eV feature to interband transitions. The shoulder on the plasmon peak may be a surface plasmon, which should occur at energies very near the bulk-plasmon loss because ϵ_1 is changing rapidly here. It may be possible to understand the shift of the plasmon to lower energy by looking at changes in the band structure. The positive potential of the hydrogen at the interstitial sites causes a lowering from 14 to 7 eV of conduction-band states near the X point of the Brillouin zone, and the appearance of a hybridized band 8 eV below E_F. Our data show the new occupied states, while evidence for the empty states comes from calculations[6] as well as x-ray absorption[37] and thermoreflectance measurements.[38] Transitions into the empty states and out of the filled states and the disappearance of lower-lying intra–d-band transitions would add oscillator strength for energies $\gtrsim 8$ eV, which would displace the zero crossing of ϵ_1 to lower energy and dampen the plasmon resonance.

B. Kinetics

The temperature dependence of the degassing pressure and hence rate of H_2 leaving the sample was found to vary with hydrogen concentration, showing two distinct regions of reversible behavior. This we will interpret to result from a depletion of β-phase material for $H_x \gtrsim 0.65$, followed by a conversion of β- into α-phase material for $H_x \lesssim 0.65$. In Fig. 5 we plot the hydrogen pressure on a log scale against reciprocal temperature. For the fully loaded sample, a completely reversible Arrhenius behavior is found with the rate $\nu^A(T) = 3\times 10^4 \exp(-4.1\times 10^3/T)$ mole $H_2\,\mathrm{sec}^{-1}$, corresponding to an activation energy of 8.1-kcal/mole H_2. This $P(T)$ relation holds provided the temperature is below 135 K and provided only a small total amount of gas has been released, otherwise the rate is considerably slower. After 15–20% of the gas has been released, the rate slows by a factor $\sim 10^5$ and becomes again reversible, following an Arrhenius behavior with the rate $\nu^B(T)=1$

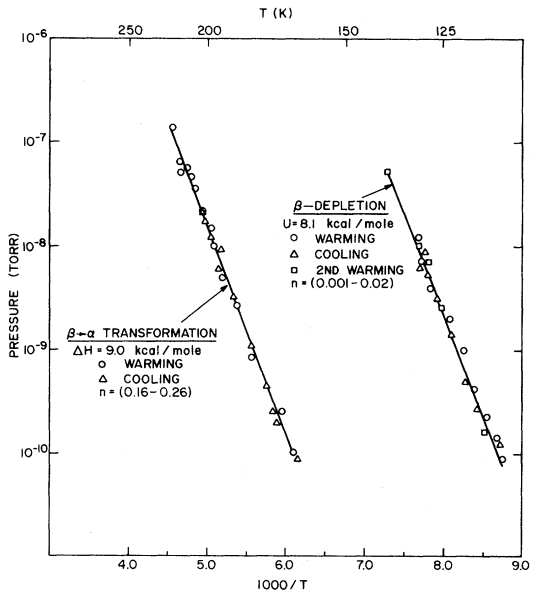

FIG. 5. Degassing pressure in the pumped chamber plotted vs reciprocal temperature. Lines are drawn through two different reversible regions showing Arrhenius behavior. The fraction n of hydrogen depleted is shown for each segment.

$\times 10^{-1}\exp(-4.5\times 10^{3}/T)$ mole $H_2\,\mathrm{sec}^{-1}$, corresponding to an activation energy of 9.0-kcal/mole H_2. With continued degassing, the rate eventually slows again, so that considerably higher temperatures are required to degas the last 20% or so of the hydrogen in a reasonable time.

The change of the core-level spectrum during degassing is shown in Fig. 6. The data were taken at 2-min intervals by repeatedly tracing the spectrum as the sample was warmed, maintaining a pressure of $\sim 5\times 10^{-8}$ Torr. We show both the FWHM and integrated intensity of the Pd $3d_{5/2}$ line calculated over an interval of 2.5 eV. The approximate hydrogen concentration in the surface region (inferred later) is shown in the upper scale. No change larger than the scatter of the data was found for a pure palladium sample over the same range of temperatures, $\sim 140-400$ K. The FWHM of the core line increases nearly linearly with the fraction of hydrogen degassed, while the data for the integrated intensity show a break near 15% depletion, changing at first rapidly and later more slowly with hydrogen depletion.

The EELS spectra at 1500-eV primary energy for several different bulk hydrogen concentrations are shown in Fig. 7. The spectra were measured at 80 K after warming to change the average hydrogen concentration to the value shown for each curve. The intensity scale has been normalized to the elastic peak in each case and does not reflect its change as hydrogen is released. The dashed line is a linear combination of curves E and B given by $0.75(E)+0.25(B)$. This sum matches very well the shape of curve D, for which the fractional degassing value n is 0.81.

We begin with a discussion of the core-level spectrum. Regardless of the detailed mechanism for the change, one may conclude immediately that since the spectrum continues to change appreciably during the entire degassing, the hydrogen concentration near the surface (20 Å) is approximately equal to that of the bulk. There is no appreciable

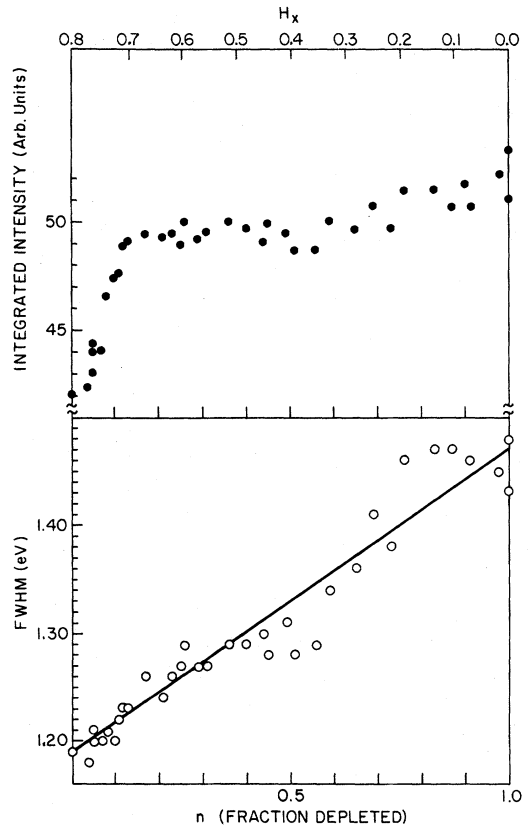

FIG. 6. Change of integrated intensity and measured width of the $3d_{5/2}$ core line as the sample is degassed. The hydrogen concentration in the surface region (see text) is shown on the upper scale.

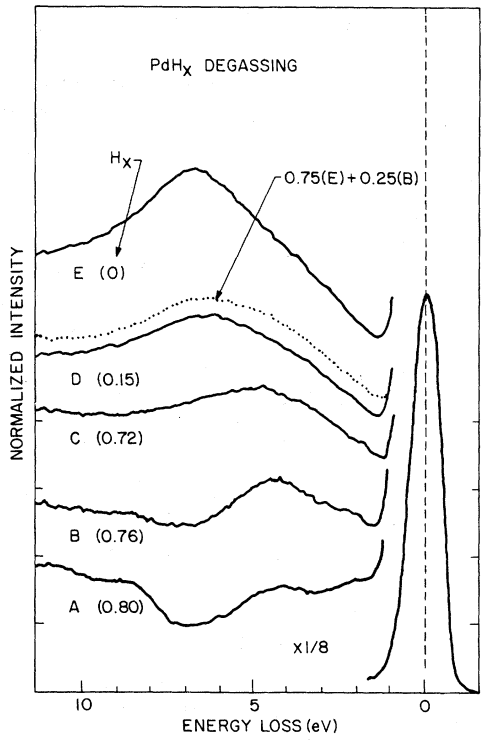

FIG. 7. EELS spectra at 1500-eV primary energy for different average hydrogen concentrations as indicated for each curve. The intensity has been normalized to the elastic peak in each case. The dotted line is the linear combination $0.75(E)+0.25(B)$, and shows that the surface contains two phases of high and low hydrogen concentrations.

surface depletion or segregation of hydrogen, at least under these conditions. This allows us to assign the H_x^{surf} values given in the figures equal to the H_x^{bulk} value as monitored by the integrated hydrogen pressure.

The break in the intensity versus concentration data near $H_x \sim 0.65$ may result from the Fermi level entering the d bands. If our suggestion that this change is due to a change in mean free path of the electron is correct, it may be puzzling to see a nonlinear dependence on hydrogen concentration. On the other hand, this may be only an artifact of the line-shape integration which was done over a limited energy range of 2.5 eV, and without deconvolution of the instrumental response. Regarding the linewidth data, one expects the asymmetry of the line to be very sensitive to the DOS near the Fermi level. That we find no break in the data is presumed due to three factors: the instrumental resolution makes up approximately half of the total width, the shakeup intensity in the asymmetric tail of the core line is determined by an integration over the joint DOS near E_F extending over a *finite* energy range, and thirdly, as explained later, the surface was found to consist of patches of α- and β-phase material for intermediate average concentrations. Since the resulting spectrum is a linear combination of signals from two phases, it would be incorrect to interpret it directly in terms of the average hydrogen concentration, as has been done in the past. A close examination of the figure shows there is possibly a break in the linewidth data for a concentration of $H_x \sim 0.25$, perhaps signifying a slight depletion of the surface layers. This coincides with the increased temperature necessary to degas the nearly empty sample, and as described later, may result from a bulk-diffusion limitation at higher temperatures, or a changing morphology of the sample.

The EELS spectra in Fig. 7 are particularly interesting since they show that for intermediate hydrogen concentration the surface consists of patches of α- (or pure palladium) and β-phase material present in a ratio approximately given by application of the lever rule between the limits of the two-phase region of the bulk-phase diagram. On the other hand, the curves for intermediate H_x are *not* obtainable by mixing curve E with curve A. This would give, for example, a very flat spectrum in the region of 7 eV which was never observed.

Knowing something about the surface hydrogen concentration, we can return to explain the $P(T)$ degassing behavior of Fig. 5. We first notice that the equilibrium pressure of H_2 over the hydride is always much larger than the actual pressure, so the reentry of hydrogen into the sample can be ignored. For the fully loaded sample we found a reversible Arrhenius behavior with a degassing rate $\nu^A(T) = 3 \times 10^4 \exp(-4.1 \times 10^3/T)$ mole $H_2\,\text{sec}^{-1}$. From Fig. 6 we know that $H_x^{surf} \approx H_x^{bulk}$, indicating a surface rate-limiting step in the degassing as opposed to a bulk-diffusion-limited process. Such a step has been previously identified in α-phase (dilute) absorption studies as being due to the $2H \rightarrow H_2$ reaction with an activation energy of ~ 7 kcal/mole.[26,27] In our experiments, H_2 is desorbing from a polycrystalline surface of β-phase material, and we find an activation energy of similar size: $U = 8.1$ kcal/mole. We can go further and at least formally determine an absolute rate constant. If we assume every surface palladium atom is an active site (i.e., a density of sites of $\sim 10^{15}/\text{cm}^2$) we obtain a rate constant of $k \sim 1 \times 10^{13} \exp(-4.1 \times 10^3/T)$ sec^{-1} for the presumed $2H \rightarrow H_2$ surface reaction.

For lower concentrations, the bulk average hydrogen concentration is within the two-phase region of the phase diagram, and the degassing rate is given by $\nu^B(T) = 1 \times 10^{-1} \exp(-4.5 \times 10^3/T)$ mole $H_2\,\text{sec}^{-1}$. Since this is 10^{-5} slower than in the high-concentration region, we believe it reflects a different rate-limiting mechanism and presume this to be the conversion of β-phase into α-phase material. The rate would then be proportional to an "internal pressure" whose temperature dependence is given by the heat of formation of the β phase. This is $\Delta H = 9.8$ kcal/mole above room temperature and somewhat smaller at lower temperatures.[39,40] This is in striking agreement with the "activation energy" we find: $U = 9.0$ kcal/mole, measured near 200 K. Presumably the effective prefactor in the degassing rate $\nu^B(T)$ is determined by the morphology of particles of β-phase material which would vary with the sample and its loading and, to a lesser extent, also the degassing conditions. A changing morphology may then explain the reduced pressure for a nearly empty sample.

It was mentioned that the degassing rate for a fully loaded sample falls below the $\nu^A(T)$ relation for temperatures above 135 K. This probably results from a diffusion-limited transport of hydrogen to the surface. One can estimate the rate of depletion of the sample from an approximate one-dimensional solution of the diffusion equations,

$$z_0(t,T) = \sqrt{D(T)t}\ , \tag{1}$$

where z_0 is the depth at which the hydrogen con-

centration is an average of its boundary values, and $D(T)$ is the diffusion constant. The degassing rate then is roughly proportional to $dz_0/dt = \frac{1}{2}D(T)/z_0(t)$. At a temperature of 180 K and a concentration of $n \sim 0.70$, we found a pressure of 1×10^{-8} Torr. Assuming that under these conditions $z_0 = 5\times10^{-4}$ cm (half of the total sample thickness), and $D \sim 10^{-8}$ cm^2 sec^{-1}, we calculate $P \sim 10^{-7}$ Torr for the diffusion process, which is the right order of magnitude to account for the experimental result.

IV. SUMMARY AND CONCLUSION

We have shown that it is possible to produce a clean palladium hydride sample with hydrogen concentration $H_x \sim 0.80$ by *in situ* loading and cleaning and cooling to liquid-nitrogen temperature. A good qualitative agreement between the valence-band spectrum and the DOS from recent band-structure calculations is found. The *d* bands "sink" in energy and narrow slightly, and a new band of states with substantial *d* character appears around 8 eV. A discrepancy with earlier UPS spectra presumably results from the greater influence of contamination in those experiments. In fact, a recent photoemission study on samples prepared similar to ours reports hydrogen-induced states at 8 eV in UPS spectra, as well as complete agreement in their XPS valence-band spectra and core-level shifts.[41]

Changes in the valence-band structure are reflected in the core-level line shape of the hydride by a suppression of the asymmetric tail and shake-up satellite due to a filling of the *d* bands. In this context, palladium is an interesting intermediate case between nickel and copper, which show, respectively, very large and nearly zero shake-up features. The disappearance of these features in the hydride, where the Fermi level is only ~ 0.1 eV above the top of the *d* bands is dramatic evidence of the importance in the shake-up process of the unoccupied *d* levels in the ground state of the system.

In the EELS spectrum a 7-eV plasmon-loss feature is damped and shifted to 5 eV, possibly due to enhanced interband transitions involving the hydrogen-induced levels. This case differs from titanium where the plasmon energy and its change in the hydride are approximately given by the simple free-electron relation $\hbar\omega_p = 4\pi ne^2/m$.[42] In the case of palladium, this calculation gives free-electron densities of $\sim\frac{1}{2}$ and $\frac{1}{4}$ electrons per Pd atom for the metal and hydride, respectively. A straightforward calculation of ϵ_2 from the band structure and of $\mathrm{Im}(1/\epsilon)$ would be useful in interpreting the results. The problem is interesting since the addition of hydrogen may be viewed as a perturbation to the complicated dielectric response of a narrow-band metal. In this context, a range of hydrogen concentrations would be desirable. This could be measured perhaps in reflectivity or ellipsometry experiments which could be done below 11 eV in a windowed system under pressure sufficient to avoid the two-phase region of the phase diagram.

Regarding the kinetics, we find that the behavior varies with temperature and hydrogen concentration. For temperatures below 135 K and a fully loaded sample (β-phase material), the degassing rate is limited by a surface reaction, presumably $2H \rightarrow H_2$, with an activation energy of 8.1-kcal/mole H_2. This energy is somewhat larger than the $\sim$7-kcal/mole H_2 found with other techniques for α-phase samples. A rate constant of $k = 1\times10^{13}\exp(-4.1\times10^3/T)$ sec^{-1} is found, assuming every surface atom is active and assuming a negligible entropy term. A prefactor in the range of phonon frequencies is considered reasonable. At temperatures above 135 K, the rate is much slower, presumably limited by diffusion through the bulk. The dominance of the bulk diffusion process at higher temperatures even though it is unimportant at lower temperatures is possible because the activation energy for diffusion is only $\sim$5-kcal/mole H,[29] thus it changes much more slowly with temperature than the surface reaction rate.

After degassing $\sim 15\%$ of the hydrogen, the sample enters the two-phase region of the composition phase diagram, and the degassing rate is 10^5 slower. The pressure now is determined by the rate of conversion of β-phase into α-phase material, which is slower than either the bulk diffusion or the surface reaction. During this time, the surface (as well as the bulk) consists of regions of both phases. This is an interesting result since it shows that the free surface does not nucleate the formation of α-phase material. Similar behavior is found in the oxidation of metals and in titanium deuteride, but is surprising here in view of the high mobility of hydrogen in palladium.[43,44] Perhaps the degassing begins at grain boundaries or other extended defects in the bulk.

Further study of both the electronic structure and kinetics on single-crystal samples would be worthwhile. Angle-resolved photoemission allows a stringent comparison of experiment with band-structure calculations, giving information that com-

plements de Haas—van Alphen and specific-heat data which only probe states at the Fermi energy. The disorder broadening of electronic states due to random occupation of the interstitial sites would also be interesting to characterize.[6] A study of the kinetic behavior on a single-crystal surface would allow connection with calculations and modeling of the detailed mechanism of the $H_2 \leftrightarrow 2H$ reaction and the trajectory of hydrogen atoms in going from the gas phase into the solid solution. The preparation of single-crystal, concentrated (i.e., β-phase) PdH_x samples for study with UHV techniques is difficult, however, because the strain induced by the 10% volume mismatch between β and α phases can crack or deform the sample. One can load a sample proceeding around the two-phase region if 20-atm pressure is available, but any subsequent release of gas at low temperatures will induce damage. The problem can perhaps be avoided using thin films where strain is more easily relieved, and also because a depression of the critical pressure has been reported for thin films.[45] Evaporated films on a metallic substrate are particularly interesting in view of their use as a hydrogen permeation coating. Here, the role of intermetallic compound formation at the surface could prove important.[46]

ACKNOWLEDGMENTS

We thank Professor M. Campagna for his continued support of this work. We are also grateful for discussions with J. M. Welter, B. Lengeler, and W. Pesch as well as technical assistance from J. Keppels.

*Present address: Bell Laboratories, Murray Hill, NJ 07974.

[1]A. C. Switendick, in *Hydrogen in Metals,* edited by G. Alefeld and J. Völkl (Springer, New York, 1978), Chap. 5.

[2]J. H. Weaver, J. A. Knapp, D. E. Eastman, D. T. Peterson, and C. B. Satterthwaite, Phys. Rev. Lett. 39, 639 (1977).

[3]J. H. Weaver, D. T. Peterson, and R. L. Benbow, Phys. Rev. B 20, 5301 (1979).

[4]D. Eastman, J. Cashion, and A. Switendick, Phys. Rev. Lett. 27, 35 (1971).

[5]P. Jena, F. Y. Fradin, and D. E. Ellis, Phys. Rev. B 20, 3543 (1979).

[6]D. Gelatt, H. Ehrenreich, and J. Weiss, Phys. Rev. B 17, 1940 (1978).

[7]J. S. Faulkner, Phys. Rev. B 13, 2391 (1976).

[8]B. W. Veal, D. J. Lam, and D. G. Westlake, Phys. Rev. B 19, 2856 (1979).

[9]F. Antonangelli, A. Balzarotti, A. Bianconi, E. Burattini, P. Perfetti, and N. Nistico, Phys. Lett. 55A, 309 (1975).

[10]P. Légaré, L. Hilaire, and G. Maire, Surf. Sci. 107, 533 (1981).

[11]S. Hüfner and G. Wertheim, Phys. Lett. 51A, 299 (1975).

[12]L. A. Feldkamp and L. C. Davis, Phys. Rev. B 22, 3644 (1980).

[13]A. Liebsch, Phys. Rev. Lett. 43, 1431 (1979); Phys. Rev. B 23, 5203 (1981).

[14]F. U. Hillebrecht, J. C. Fuggle, P. Bennett, Z. Zolnierek, and Ch. Freiburg, Phys. Rev. B (in press).

[15]J. C. Fuggle and Z. Zolnierek, Solid State Commun. 38, 799 (1981).

[16]P. O. Nilsson, C. G. Larsson, and W. Eberhardt, Phys. Rev. B 24, 1739 (1981).

[17]S. Doniach and M. Sunjic, J. Phys. C 3, 285 (1970).

[18]G. K. Wertheim and P. H. Citrin, in *Photoemission in Solids,* edited by M. Cardonna and L. Ley (Springer, Berlin, 1978), Chap. 5.

[19]F. Antonangelli, A. Balzarotti, A. Bianconi, P. Perfetti, P. Ascarelli, and N. Nistico, Nuovo Cimento B 39, 720 (1977).

[20]J. H. Weaver, Phys. Rev. B 11, 1416 (1975).

[21]J. Daniels, C. V. Festenberg, H. Raether, and K. Zeppenfeld, in *Optical Constants by Electron Spectroscopy,* Vol. 54 of *Springer Tracts in Modern Physics,* edited by G. Hohler (Springer, New York, 1970).

[22]R. Lässer and N. V. Smith, Phys. Rev. B 25, 806 (1982).

[23]R. Wiswall, in *Hydrogen in Metals II,* edited by G. Alefeld and J. Völkl (Springer, New York, 1978), Chap. 5.

[24]M. Strongin, M. El-Batanouny, and M. Pick, Phys. Rev. B 22, 3126 (1980).

[25]L. Schlapbach, A. Seiler, H. C. Siegmann, T. Waldkirsch, P. Zurcher, and C. R. Brundle, *Hydrogen Energy System* (Pergamon, New York, 1979), Sec. V.

[26]W. Auer and H. J. Grabke, Ber. Bunsenges. Phys. Chem. 78, 58 (1974).

[27]E. Wicke and K. Meyer, Z. Phys. Chem. Neue Folge 64, 225 (1969).

[28]S. Hüfner and G. Wertheim, Phys. Lett. 47A, 349 (1974).

[29]E. Wicke and H. Brodowsky, in *Hydrogen in Metals II,* edited by G. Alefeld and J. Völkl (Springer, New York, 1978), Chap. 3.

[30]I. S. Anderson, C. J. Carlile, and D. K. Ross, J. Phys. C 11, L381 (1978).

[31]J. H. Scofield, J. Electron Spectrosc. 8, 129 (1976).

[32]J. C. Fuggle and D. Menzel, Surf. Sci. 53, 21 (1975).
[33]J. C. Fuggle, T. E. Madey, M. Steinkilberg, and D. Menzel, Phys. Lett. 51A, 163 (1975).
[34]J. C. Fuggle and D. Menzel, Chem. Phys. Lett. 33, 37 (1975).
[35]S. Louie, Phys. Rev. Lett. 42, 476 (1979).
[36]J. E. Demuth, Surf. Sci. 65, 369 (1977).
[37]E. Gilberg, *Proceedings of the 5th International Conference on the Physics of X-ray Spectra* (U.S. GPO, Washington, D.C., 1976), p. 229.
[38]G. A. Frazier and R. Glosser, Solid State Commun. 41, 245 (1982).
[39]H. Frieske and E. Wicke, Ber. Bunsenges. Phys. Chem. 77, 50 (1973).
[40]J. D. Clewley, T. Curran, T. B. Flanagan, and W. A. Oates, J. Chem. Soc. Faraday Trans. I 69, 449 (1973).
[41]L. Schlapbach and J. P. Burger, J. Phys. Lett. (Paris) 43, L273 (1982).
[42]B. C. Lamartine, T. W. Haas, and J. S. Solomon, Appl. Surf. Sci. 4, 537 (1980).
[43]P. Holloway, J. Vac. Sci. Technol. 18, 653 (1981).
[44]M. E. Malinowski, J. Vac. Sci. Technol. 16, 962 (1979).
[45]G. J. de Bruin-Hordijk, R. Feenstra, H. L. M. Bakker, D. G. de Groot, and R. Griessen, in Proceedings of the Nato International Symposium on the electronic Structure and Properties of Hydrogen in Metals, Richmond, Virginia, 1980 (Plenum, New York, in press).
[46]M. El-Batanouny, M. Strongin, G. P. Williams, and J. Colbert, Phys. Rev. Lett. 46, 269 (1981); S. Lin-Weng and M. El-Batanouny, *ibid.* 44, 612 (1980).